# Biochemical and Structural Analysis of 14 Mutant ADSL Enzyme Complexes and Correlation to Phenotypic Heterogeneity of Adenylosuccinate Lyase Deficiency

**ARTICLE** *in* HUMAN MUTATION · APRIL 2010

Impact Factor: 5.14 · DOI: 10.1002/humu.21212 · Source: PubMed



**5 AUTHORS**, INCLUDING:

Marie Zikánová
Charles University in Prague
**16** PUBLICATIONS **213** CITATIONS
SEE PROFILE

Vaclava Skopova
Charles University in Prague
**6** PUBLICATIONS **42** CITATIONS
SEE PROFILE

Ales Hnizda
Academy of Sciences of the Czech Republic
**14** PUBLICATIONS **125** CITATIONS
SEE PROFILE

Jakub Krijt
Charles University in Prague
**82** PUBLICATIONS **1,024** CITATIONS
SEE PROFILE

RESEARCH ARTICLE

Human Mutation

OFFICIAL JOURNAL
HGVS
HUMAN GENOME VARIATION SOCIETY
www.hgvs.org

# Biochemical and Structural Analysis of 14 Mutant ADSL Enzyme Complexes and Correlation to Phenotypic Heterogeneity of Adenylosuccinate Lyase Deficiency

Marie Zikanova, Vaclava Skopova, Ales Hnizda, Jakub Krijt, and Stanislav Kmoch*

*Institute of Inherited Metabolic Disorders, Charles University in Prague, First Faculty of Medicine, Prague, Czech Republic*

Communicated by Hans R. Waterham

Received 6 November 2009; accepted revised manuscript 19 January 2010.
Published online 2 February 2010 in Wiley InterScience (www.interscience.wiley.com). DOI 10.1002/humu.21212

**ABSTRACT:** Adenylosuccinate lyase (ADSL) deficiency is neurometabolic disease characterized by accumulation of dephosphorylated enzyme substrates SAICA-riboside (SAICAr) and succinyladenosine (S-Ado) in body fluids of affected individuals. The phenotypic severity differs considerably among patients: neonatal fatal, severe childhood, and moderate phenotypic forms correlating with different values for the ratio between S-Ado and SAICAr concentrations in cerebrospinal fluid have been distinguished. To reveal the biochemical and structural basis for this phenotypic heterogeneity, we expressed and characterized 19 ADSL mutant proteins identified in 16 patients representing clinically distinct subgroups. Respecting compound heterozygosity and considering the homotetrameric structure of ADSL, we used intersubunit complementation and prepared and characterized genotype-specific heteromeric mutant ADSL complexes. We correlated clinical phenotypes with biochemical properties of the mutant proteins and predicted structural impacts of the mutations. We found that phenotypic severity in ADSL deficiency is correlated with residual enzymatic activity and structural stability of the corresponding mutant ADSL complexes and does not seem to result from genotype-specific disproportional catalytic activities toward one of the enzyme substrates. This suggests that the S-Ado/SAICAr ratio is probably not predictive of phenotype severity; rather, it may be secondary to the degree of the patient's development (i.e., to the age of the patient at the time of sample collection).
Hum Mutat 31:445–455, 2010. © 2010 Wiley-Liss, Inc.

**KEY WORDS:** adenylosuccinate lyase; ADSL deficiency; phenotype heterogeneity; de novo purine synthesis; purine nucleotide cycle; intersubunit complementation

## Introduction

Adenylosuccinate lyase (ADSL; EC 4.3.2.2.) is an enzyme acting in two pathways of purine nucleotide metabolism. It catalyzes the conversion of succinylaminoimidazole carboxamide ribotide (SAICAR) into aminoimidazole carboxamide ribotide (AICAR) in the purine de novo synthesis pathway and the formation of adenosine monophosphate (AMP) from adenylosuccinate (S-AMP) in the purine nucleotide cycle (Fig. 1) [Ciardo et al., 2001; Jaeken and Van den Berghe, 1984].

ADSL functions in the form of a homotetrameric complex. The ADSL subunits are encoded in humans by a single *ADSL* gene (MIM# 608222), which spans 23 kb on chromosome 22q13.1–13.2. The gene consists of 13 exons, and it is ubiquitously expressed as two alternatively spliced mRNA isoforms [Fon et al., 1993; Kmoch et al., 2000; Van Keuren et al., 1987].

Mutations in the *ADSL* gene that compromise enzyme functions lead to an autosomal recessive neurometabolic disease called ADSL deficiency (MIM# 103050) [Jaeken and Van den Berghe, 1984]. To date, about 60 patients with ADSL deficiency and 45 different disease-causing *ADSL* mutations have been reported [Gitiaux et al., 2009; Jurecka et al., 2008; Mouchegh et al., 2007; Spiegel et al., 2006]. Enzyme deficiency leads to the intracellular accumulation of SAICAR and S-AMP, which are consequently dephosphorylated intracellularly to SAICA-riboside (SAICAr) and succinyladenosine (S-Ado), respectively (Fig. 1). These metabolites are excreted from cells and are present in the plasma, urine, and cerebrospinal fluid of affected individuals at concentrations exceeding two orders of magnitude greater than those observed in healthy individuals [Krijt et al., 1999].

The patients manifest clinically mostly within the first year of life with psychomotor retardation, seizures, hypotonia, growth retardation, muscular wasting and, interestingly, a wide spectrum of behavioral changes such as autism, aggressiveness, and self-mutilation. The age of onset, severity, and combinations of different symptoms vary among patients, and three distinct clinical phenotypes have been distinguished:

1. The neonatal fatal form presenting with prenatal hyperkinesias, pulmonary hypoplasia and prenatal growth restriction, resulting in fatal neonatal encephalopathy [Mouchegh et al., 2007];
2. The severe childhood form (type I) presenting within the first months of life, encompassing the whole spectrum of disease symptoms and resulting in severe psychomotor retardation, developmental arrest, coma vigil, and often early death [Jaeken et al., 1988; Maaswinkel-Mooij et al., 1997];
3. The moderate or mild form (type II) presenting within the first years of life either with psychomotor retardation or hypotonia [Jaeken et al., 1988, 1992; Krijt et al., 1999; Valik et al., 1997].

The pathogenic mechanism(s) leading to the development of individual clinical symptoms and underlying the phenotypic heterogeneity remain(s) unclear.

Additional Supporting Information may be found in the online version of this article.

*Correspondence to: Stanislav Kmoch, Institute of Inherited Metabolic Disorders, Ke Karlovu 2, 128 00 Prague 2, Czech Republic. E-mail: skmoch@lf1.cuni.cz

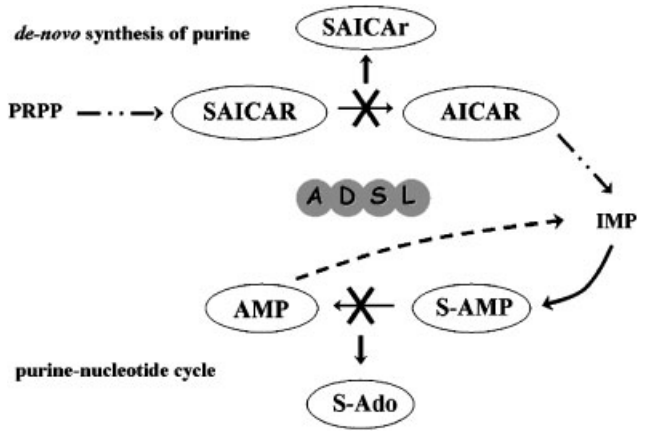


**Figure 1.** A scheme of ADSL functions in de novo purine synthesis pathway and purine nucleotide cycle. Corresponding enzymatic defects are demonstrated by crosses and alternative metabolic routes leading to SAICAr and S-Ado are depicted. PRPP, phosphoribosyl pyrophosphate; AICAR, aminoimidazole carboxamide ribotide; IMP, inosine monophosphate.

The hypothesis of systemic purine nucleotide deficiency was tested but not proven by several experiments investigating either the rate of de novo purine synthesis in fibroblasts [Van den Bergh et al., 1993] or measuring purine nucleotide concentrations in tissues of ADSL-deficient patients [Van den Berghe and Jaeken, 1986].

The main pathogenic effect, therefore, has been attributed to the toxic effects of accumulating succinylpurines [Stone et al., 1998]. Although the absolute S-Ado and SAICAr concentrations in body fluids do not correlate with the severity of the phenotype, it has been found that different values for the ratio between S-Ado and SAICAr concentrations in cerebrospinal fluid (S-Ado/SAICAr ratio) do correspond with the three main phenotypic groups [Mouchegh et al., 2007; Van den Bergh et al., 1993]:

1. In patients with the neonatal fatal form, the S-Ado/SAICAr ratio is less than 1;
2. In patients with the severe childhood form, the S-Ado/SAICAr ratio is close to 1;
3. In patients with the moderate or mild form, the S-Ado/SAICAr ratio is more than 2.

The mechanism(s) leading to this diversity in S-Ado/SAICAr ratios is (are) not clear. As native ADSL functions in the form of a homotetrameric complex with four active sites, each of which is formed by three different subunits [Ariyananda Lde et al., 2009], it can be hypothesized that these differences in the S-Ado/SAICAr ratio may be genotype-specific and structure-related nonparallel loss (or gain) of activity toward one of the enzyme substrates.

To test this hypothesis we recently cloned, expressed, purified, and biochemically characterized recombinant human wild-type ADSL and its seven mutant forms—c.8C>T (p.Ala3Val), c.340T>C (p.Tyr114His), c.569G>A (p.Arg190Gln), c.580C>T (p.Arg194Cys), c.802G>A (p.Asp268Asn), c.1277G>A (p.Arg426His), and c.1288G>A (p.Asp430Asn)—identified in six ADSL-deficient patients. We confirmed the pathogenicity of the individual mutations and identified the underlying structural and/or catalytic basis of the enzyme deficiency. We also assessed genotype–phenotype correlations and observed that the predicted residual enzyme activity of the individual genotypes (calculated as the mean of the homoallelic in vitro activity) correlates with the severity of the phenotype (e.g., different S-Ado/SAICAr ratios). Nevertheless, we found that all of the mutant proteins displayed a proportional decrease in activity toward both substrates; therefore, no reasons for the different S-Ado/SAICAr ratios were identified [Kmoch et al., 2000].

Our "single-protein" focused studies, however, did not take into account the fact that the patients are mostly compound heterozygotes and that two structurally different mutant enzymes are involved in the tetrameric structure in vivo. In this process, both mutant proteins may recombine randomly to form any of five possible tetrameric structures with different active sites. It is conceivable that some of these heteromeric mutant complexes may form unique catalytic sites or substrate channels, leading to disproportional activity and selectivity toward one of the enzyme substrates. In parallel, this process can also significantly affect the stability and activity of the mutant enzyme complexes, contributing to any related phenotypic severity.

The process of random oligomerization can be tested in vitro using intersubunit complementation in which the individual subunits are either mixed or preferably coexpressed together before further characterization [Brosius and Colman, 2002; Lee et al., 1999; Yu and Howell, 2000].

To test this hypothesis and approach and to corroborate our previous observation of the correlation of residual enzyme activity with phenotypic severity, we selected 16 ADSL-deficient patients who, as defined by clinical presentation and different S-Ado/SAICAr ratios, presented with the neonatal fatal form (five cases), the severe childhood form (five cases), or the moderate or mild form (six cases). We identified individual disease-causing genotypes and cloned individual mutations into expression vectors with ampicillin and kanamycin resistance. We then expressed individual mutant proteins and coexpressed genotype-specific mutant proteins in *Escherichia coli*. Following affinity purification of recombinant proteins, we reconstituted both homomeric complexes (composed of a single mutant protein) and heteromeric complexes (composed from two genotype specific mutant proteins) at 25 and 50°C and characterized and compared their biochemical properties. Furthermore, we located selected mutations in the available structural model of the human ADSL complex and correlated their positional effects with experimentally obtained biochemical characteristics of the homomeric and heteromeric enzyme complexes and corresponding phenotypic severity.

## Materials and Methods

### Selection of ADSL Phenotypes and Related Mutations

Clinical, biochemical, and molecular data on ADSL patients were available to us either from our previous studies [Jurecka et al., 2008; Kmoch et al., 2000; Mouchegh et al., 2007] or compiled from the literature and existing databases (http://www.icp.ucl.ac.be/adsldb). The nucleotide numbering corresponds to the cDNA sequence deposited in GenBank under accession AF067853.1. According to journal guidelines, the A of the ATG translation initiation codon in the reference sequence is numbered as +1 (http://www.hgvs.org/mutnomen). The amino acid residues are numbered from the N-terminus starting with initiation ATG codon.

### Preparation of Ampicillin-Resistant ADSL Expression Vectors

The expression vectors pMAL–c2wtADSL and pMAL–c2 with *ADSL* mutants c.69C>G (p.Ser23Arg), c.340T>C (p.Tyr114His),

c.569G>A (p.Arg190Gln), c.580C>T (p.Arg194Cys), c.643G>C (p.Asp215His), c.725C>T (p.Thr242Ile), c.802G>C (p.Asp268His), c.1052T>C (p.Ile351Thr), c.1128G>C (p.Glu376Asp), c.1186C>T (p.Arg396Cys), c.1277G>A (p.Arg426His), and c.1288G>A (p.Asp430Asn) and ampicillin resistance (ampR) from the original pMAL–c2 vector (NEB, Frankfurt am Main, Germany) were available to us from our previous studies [Jurecka et al., 2008; Kmoch et al., 2000; Mouchegh et al., 2007]. We introduced the mutations c.240A>C (p.Glu80Asp), c.261T>G (p.Asp87Glu), c.907C>T (p.Arg303Cys), c.1187G>A (p.Arg396His), and c.1349C>G (p.Thr450Ser) into the pMAL–c2wtADSL vector using site-directed mutagenesis with mutation specific oligonucleotide primers and the GeneTailor™ Site-Directed Mutagenesis System Kit (Invitrogen, Paisley, UK).

## Preparation of Kanamycin-Resistant ADSL Expression Vectors

To prepare the pMAL–c2 vector with kanamycin resistance, we first PCR amplified the kanamycin resistance (*kanR*) fragment present in the pCR®–XL-TOPO® plasmid (Invitrogen). We then replaced the original *ampR* region in pMAL–c2–Arg426His-ADSL with the *kanR* fragment using BspHI restriction sites (Fermentas, St. Leon-Rot, Germany). *ADSL* mutations encoding p.Glu80Asp, p.Tyr114His, p.Asp215His, and p.Arg396Cys were subcloned into the pMAL–c2–Arg426His–ADSLkan vector from the corresponding pMAL–c2 mutant ADSL vectors using SacI and XbaI (Fermentas) restriction sites.

## Expression, Coexpression, and Affinity Purification of the Recombinant Proteins

We introduced all of the sequence-verified vectors into DH5αF′IQ competent cells (NEB) and expressed recombinant maltose binding protein–ADSL fusion proteins (MBP–ADSL) as previously described [Kmoch et al., 2000].

For coexpression of the genotype-specific mutant proteins, we transformed DH5αF′IQ competent cells with the corresponding ampR and kanR vectors. We confirmed the presence of both vectors in selected bacterial clones by DNA sequencing. To achieve approximately equal representation of both DNA constructs we optimized kanamycin concentrations in the cultures accordingly to the fluorescent signal from the ALFExpress DNA analyzer (Table 1). The ampicillin concentration in the cultivation medium was kept at 50 μg/ml in all expression experiments. Both mutant fusion proteins were coexpressed as described above.

The resulting MBP–ADSL fusion proteins were isolated from the crude bacterial lysates using high-flow amylose resin (NEB) affinity columns. The ADSL proteins were released from the MBP fusion directly on the column using factor Xa (Qiagen, Hilden, Germany) and then eluted using ADSL buffer (10 mM Tris, pH 8, 2 mM EDTA, 10 mM KCl, 1 mM DTT, 4% glycerol). Protein concentrations in the eluate were determined using the Bradford assay (Sigma-Aldrich, Prague, Czech Republic). We diluted the purified proteins with ADSL buffer to a final concentration of 250 μg/ml and assessed protein production using SDS-PAGE analysis. Protein complexes were reconstituted and equilibrated at 25 and 50°C for 2 hr before further characterization.

## Mass Spectrometry Analysis

We confirmed the presence of both mutant proteins in the resulting heteromeric complexes by mass spectrometry. We dialyzed the protein complexes against 50 mM $NH_4HCO_3$ using Slide Lyzer Units (Thermo Fisher Scientific, Waltham, MA) for 2 hr and reduced them with 5 mM DTT for 30 min at 50°C. Reduced cysteines were acetamidated using IAA for 30 min in the dark at room temperature. We digested the protein preparations with trypsin, chymotrypsin, Asp-N, or Lys-C for 2 hr at 37°C using protein: enzyme ratios of 1:20 (w/w; for trypsin and chymotrypsin) and 1:100 (w/w; for Asp-N and Lys-C).

We mixed the protein digest with matrix solution (a saturated solution of α-cyano-4-hydroxycinnamic acid with a sample:matrix ratio of 1:3.5) and analyzed it using an Autoflex II (Bruker Daltonics, Brno, Czech Republic) mass spectrometer equipped

**Table 1. Clinical and Biochemical Presentation of Selected ADSL Mutations Characterized in This Study**

| Phenotype | SAdo/SAICAr in CSF | Mutation 1 KanR | Mutation 2 AmpR | Kan[b] μg/ml | Stability at 50°C BN-PAGE[c] |
|---|---|---|---|---|---|
| neonatal[a] | 0.5 | c.1277G>A (p.Arg426His)[d] | c.340T>C (p.Tyr114His) | 200 | 0.5 |
| neonatal | 0.6 | p.Tyr114His | c.1128G>C (p.Glu376Asp) | 425 | 0.5 |
| neonatal | 0.7 | p.Tyr114His | c.1186C>T (p.Arg396His) | 400 | 0.5 |
| neonatal | n.d. | c.1186C>T (p.Arg396Cys) | c.580C>T (p.Arg194Cys) | 450 | 1 |
| neonatal/type I[a] | 0.9 | p.Tyr114His | c.725C>T (p.Thr242Ile) | 525 | 0.5 |
| type I | 0.8 | p.Arg426His | c.69C>G (p.Ser23Arg) | 175 | 0.5 |
| type I | 1.0 | p.Asp268Asn | p.Arg194Cys | | |
| type I | n.d. | c.1400C>G (p.Pro467Arg) | c.802G>A (p.Asp268Asn) | | |
| type I[a] | 1.3–1.7 | | p.Arg426His/p.Arg426His | | 0 |
| type I | 1.3 in urine | c.643G>C (p.Asp215His) | c.1128G>C (p.Ile351Thr) | 350 | 1 |
| type II/type I | 2.1 in urine | p.Arg426His | c.802G>C (p.Asp268His) | 475 | 0 |
| type II/type I | 2.5 | p.Arg426His | c.1349C>G (p.Thr450Ser) | 250 | 1 |
| type II[a] | 2.1–2.2 | p.Tyr114His | c.569G>A (p.Arg190Gln) | 300 | 1 |
| type II | 2.4 in urine | c.240A>C (p.Glu80Asp) | c.261T>G (p.Asp87Glu) | 350 | 1 |
| type II | 2.6 in urine | p.Arg426His | c.1288G>A (p.Asp430Asn) | 260 | 1 |
| type II[a] | 3–4 | | c.907C>T (p.Arg303Cyc)/p.Arg303Cys | | 1 |

Denotes genotypes that have been recurrently observed in patients with ADSL deficiency. Underlying genotypes are shown in the parentheses. KanR (kanamycin) and AmpR (ampicilin) denote type of antibiotic resistance present in the expression vectors.
[a]More patients with this genotype.
[b]Optimized concentration of kanamycin ensuring equal representation of both KanR and AmpR plasmids in *E. coli* is provided.
[c]Stability of heteromeric enzyme complexes equilibrated at 50°C as shown by BN-PAGE, 0 denotes unstable complexes; 0.5 denotes complexes with decreased stability; 1 enotes stable complexes.
[d]GenBank AF106656.1.

with a nitrogen laser (337 nm) in reflector positive mode (*m/z* range from 500 to 4,500).

The mass spectrometer was externally calibrated with Peptide Calibration Standard II (Bruker Daltonics). The identities of peptides carrying the point mutations were confirmed using MS/MS (method LIFT). Spectra were processed by mMass 3.0 [Strohalm et al., 2008] and Biotools 3.0, and the mass accuracy tolerance was set at 50 ppm for MS and $\pm 0.5$ Da for MS/MS analyses.

### Blue-Native Electrophoresis, Gel Filtration, and SDS-PAGE Analysis

We analyzed ADSL complexes using standard Blue native electrophoresis (BN-PAGE) with imidazole buffers [Wittig et al., 2006]. For the protein standards, we used the High Molecular Weight Calibration Kit for Electrophoresis and rabbit aldolase (GE Healthcare, Freiburg, Germany). Proteins were detected by silver staining using a Silver Sequence Kit (Promega, Mannheim, Germany).

Gel filtration was performed using a Superdex 200 (GE Healthcare) column equilibrated with TBS buffer, pH 8.0 (137 mM NaCl, 2.7 mM KCl, 24.8 mM Tris), with 0.05% mercaptoethanol. Eluted proteins were monitored using OD 280 detection.

Chemical crosslinking was performed with Bis[Sulfosuccinimidyl] glutarate-$d_0$ (Thermo Fisher Scientific), and crosslinked complexes were analyzed using 10% SDS-PAGE and detected by silver staining as described above.

### ADSL Activity Assay, HPLC Analysis

Enzyme activity was measured by HPLC analysis of AMP and AICAR formed from both ADSL substrates, S-AMP (Sigma-Aldrich) and SAICAR (for synthesis, see [Zikanova et al., 2005]). We ran the reactions for 20 min at 37°C in 65 µl ADSL buffer and 20 ng protein as previously described [Kmoch et al., 2000]. The substrate concentrations were 0.25 and 0.15 mM for S-AMP and SAICAR, respectively.

### In Silico Analysis of the ADSL 3D Structure

The structural topology of the mutations was determined using a structural model of human ADSL (crystallized with its substrate, S-AMP, and products, AMP and fumarate), which is available in the Protein Data Bank (PDB) (2VD6; http://www.pdb.org/pdb/cgi/explore.cgi?pdbId = 2VD6). Catalytic clefts and the identified mutations located in their proximity were highlighted using data from the Catalytic Site Atlas (http://www.ebi.ac.uk/thornton-srv/databases/CSA). Mutations in other regions (e.g., the substrate channel, central helical region, and subunit interface) were located as described previously [Ariyananda Lde et al., 2009]. The structural model of ADSL was visualized and analyzed using the PyMOL Viewer (http://www.pymol.org).

### Statistical Analysis

All of the statistical analyses were performed using Statistica 7.0 software (StatSoft, CR).

## Results

### Selection of Phenotypes and Mutations

We searched the available literature and databases describing patients with ADSL deficiency and retrieved the relevant clinical, biochemical, and molecular data and complementary data on ADSL patients analyzed at our institution over last the 15 years. In total, we collected information on 60 patients (http://udmp.lf1.cuni.cz/adsl). We assigned individual patients into three main phenotypic groups according to the severity of their clinical presentation and S-Ado/SAICAr ratio value in cerebrospinal fluid or urine when the former was not available. From this cohort we selected 16 genotypes representing the neonatal fatal form (five cases), the severe childhood form (five cases), and the moderate or mild form (six cases) as defined by the corresponding clinical presentation and different S-Ado/SAICAr ratios [Jurecka et al., 2008; Kmoch et al., 2000; Mouchegh et al., 2007; Race et al., 2000; Sivendran et al., 2004]. In the selection process, we preferentially chose genotypes of patients diagnosed and characterized in our institute and recurrently observed genotypes. The selected genotypes included 19 different *ADSL* mutations. A clinical presentation and brief biochemical characterization of the selected genotypes is provided in Table 1.

### Expression and Biochemical Characterization of ADSL Proteins

As showed by SDS-PAGE analysis, we were able to prepare wild-type and 17 homomeric and 12 heteromeric mutant ADSL protein complexes. We did not succeed in the coexpression of two heteromeric mutant complexes because of permanent loss of the kanamycin-resistant expression vectors encoding the p.Asp268Asn and c.1400C>G (p.Pro467Arg) mutations. The presence of both mutant proteins in the prepared heteromeric complexes was confirmed by peptide mass fingerprinting with mass spectrometric detection.

### Blue Native Gel Electrophoresis

Following equilibration at 25 and 50°C, we assessed protein complex formation using Blue native gel electrophoresis (Fig. 2). The analysis showed different mobilities of the p.Tyr114His, p.Asp215His, p.Asp268His, and p.Arg426His homomeric complexes. These mobility shifts were not caused by differences in the native molecular weight of the proteins as shown by subsequent gel filtration analysis of native protein complexes and SDS-PAGE analysis of chemically crosslinked proteins (data not shown). Furthermore, the mobility shifts were detected whenever any of these four mutant proteins was present in the heteromeric complexes.

The BN-PAGE analysis also showed the instability of p.Tyr114His, p.Asp268His, and p.Arg426His and the decreased stability of p.Ser23Arg, p.Glu80Asp, p.Arg190Gln, p.Glu376Asp, and p.Thr450Ser homomeric complexes at 50°C. A positive complementation effect demonstrated by higher thermal stability of the heteromeric complexes compared to that of the homomeric forms was observed for p.Tyr114His/p.Arg426His, p.Tyr114His/p.Glu376Asp, and p.Arg426His/p.Thr450Ser. The other heteromeric complexes showed stabilities very similar to those of the component proteins in their homomeric forms.

### Enzymatic Activity

We measured the enzymatic activity of the wild-type ADSL and homomeric and heteromeric mutant enzyme complexes reconstituted at 25 and 50°C with both ADSL substrates, S-AMP and SAICAR, at 37°C. The data are shown in Table 2 and Table 3, respectively. In Table 3, we also present the calculated ratio of SAICAR/S-AMP activity and the arithmetic mean of the corresponding homomeric enzyme activity.

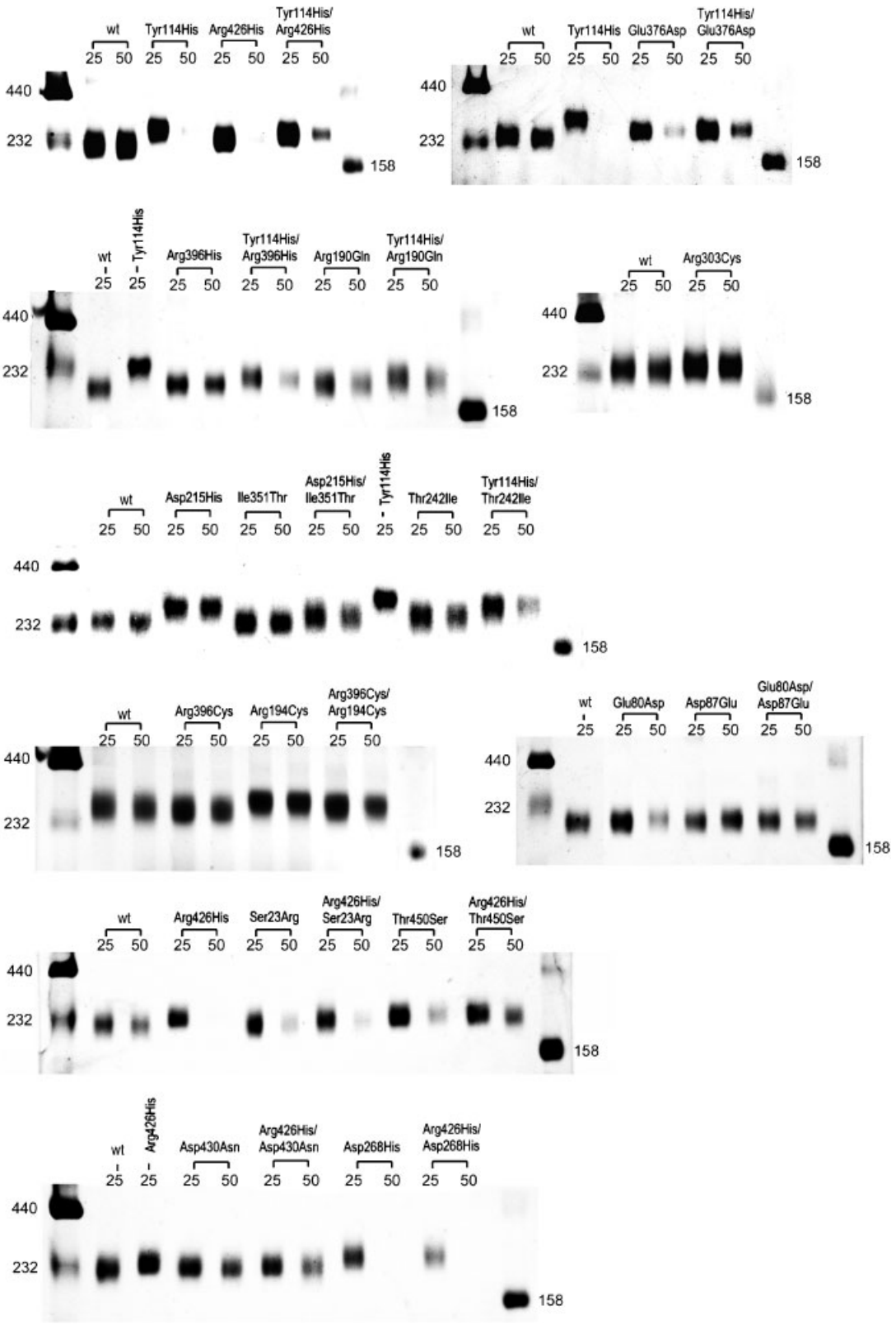


**Figure 2.** Formation and stability of ADSL protein complexes. Blue native electrophoresis gels showing molecular sizes and relative amounts of the corresponding homomeric and heteromeric enzyme complexes reconstituted at 25 or 50°C. Molecular standard sizes are shown in kDa on each side of the gel.

The measured enzyme activity of the heteromeric complexes correlated with the arithmetic mean of the corresponding homomeric enzyme activities (Pearson correlation coefficients for S-AMP and SAICAR at 25°C and S-AMP and SAICAR at 50°C were 0.86, 0.95, 0.91, and 0.94, respectively; see Supp. Fig. S1). The obtained SAICAR/S-AMP activity ratios of the heteromeric complexes were moderately correlated with the corresponding S-Ado/SAICAr ratios detected in the body fluids of the patients (Pearson correlation coefficient 0.56) (Supp. Fig. S2). Visual inspection and Spearman correlation analysis of the data, however, revealed that this correlation was mostly due to the unique properties of the p.Arg303Cys/p.Arg303Cys protein. This protein complex displayed the highest SAICAR/S-AMP activity ratio, evidently resulting from an extremely low enzyme activity with S-AMP. With regard to the other heteromeric complexes, no evidence for an altered S-Ado/SAICAr ratio was found. We tested whether the residual enzyme activity at 25°C differed among the three phenotypic groups. The Kruskal-Wallis test was significant ($P \leq 0.05$); however, a post hoc paired comparison showed no significant difference among the three groups. Visual inspection of the data revealed that the heteromeric complexes associated with the neonatal fatal form tended to have lower residual activity comparable to the complexes associated with the type I and type II phenotypes, which had similar activity. When we aggregated the residual activity of the heteromeric complexes associated with the type I and type II phenotypes and compared them to the heteromeric complexes associated with the neonatal fatal form, the difference was significant (Mann-Whitney test, $P \leq 0.05$; Fig. 3).

**Table 2. Enzymatic Activities of Homomeric Mutant Enzyme Complexes**

| Homomeric proteins | SAMP | | SAICAR | |
|---|---|---|---|---|
| M amp | 25°C | 50°C | 25°C | 50°C |
| wt | 100±30 | 84±29 | 100±34 | 79±26 |
| p.Ser23Arg | 73±21 | 28±20 | 108±38 | 44±18 |
| p.Glu80Asp | 100±13 | 85±21 | 102±24 | 79±21 |
| p.Asp87Glu | 95±18 | 114±15 | 91±23 | 89±17 |
| p.Tyr114His | 28±16 | 3±5 | 37±7 | 6±8 |
| p.Arg190Gln | 158±41 | 150±11 | 119±26 | 121±30 |
| p.Arg194Cys | 141±45 | 105±31 | 101±9 | 82±25 |
| p.Asp215His | 108±24 | 108±19 | 92±23 | 83±20 |
| p.Thr242Ile | 112±10 | 93±6 | 108±13 | 86±17 |
| p.Asp268His | 6±4 | 11±11 | 20±13 | 8±6 |
| p.Arg303Cys | 18±1 | 20±2 | 44±13 | 43±9 |
| p.Ile351Thr | 170±38 | 157±27 | 151±53 | 115±25 |
| p.Glu376Asp | 53±15 | 20±8 | 49±12 | 20±7 |
| p.Arg396Cys | 15±2 | 17±10 | 32±14 | 17±8 |
| p.Arg396His | 10±3 | 9±2 | 18±4 | 18±7 |
| p.Arg426His | 92±30 | 12±11 | 89±30 | 11±10 |
| p.Asp430Asn | 139±32 | 96±9 | 151±50 | 100±42 |
| p.Thr450Ser | 82±18 | 14±3 | 68±12 | 18±6 |

Complexes were reconstituted at 25°C and 50°C and measured with both of ADSL substrates, S-AMP and SAICAR, at 37°C. Mutations are ordered according to their position in ADSL sequence. Relative activities - %wt at 25°C.

## Structural Analysis of the ADSL Mutations

Using the crystal structure of wtADSL, we located six "active site" mutations (p.Glu80Asp, p.Asp87Glu, p.Tyr114His, p.Thr242Ile, p.Asp268Asn, and p.Arg303Cys), six "substrate channel" mutations (p.Asp215His, p.Arg396Cys, p.Arg396His, p.Arg426His, p.Asp430Asn, and p.Thr450Ser), one mutation located in the central helical region (p.Arg190Gln) and one mutation at a subunit interface (p.Arg194Cys). Two mutations were found at the interface of a helical region with active sites (p.Ser23Arg, p.Ile351Thr), and one mutation was located in proximity to the catalytic cleft participating in interactions between subunits (p.Glu376Asp).

## Functional–Structural Correlation of Homomeric Complexes

Enzyme activity measurements in homomeric complexes have defined four classes of proteins: (1) a single protein p.Arg303Cys with a disproportional decrease in activity toward S-AMP

**Table 3. Enzymatic Activities of Heteromeric Mutant Enzyme Complexes**

| | Heteromeric mutant proteins M1kan/M2 amp | S-AMP 25°C | | SAICAR 25°C | | SAICAR/S-AMP 25°C | SAMP 50°C | | SAICAR 50°C | | SAICAR/S-AMP 50°C |
|---|---|---|---|---|---|---|---|---|---|---|---|
| | | measured | calc[b] | measured | calc | measured | measured | calc | measured | calc | measured |
| | wt/wt[a] | 100±30 | | 100±34 | | | 84±29 | | 79±26 | | |
| Neonatal | p.Arg426His/p.Tyr114His | 63±23 | 60 | 75±11 | 63 | 1.2 | 10±8 | 7 | 11±5 | 9 | 1.1 |
| | p.Tyr114His/p.Glu376Asp | 51±7 | 41 | 42±8 | 43 | 0.8 | 50±7 | 11 | 33±7 | 13 | 0.7 |
| | p.Tyr114His/p.Arg396His | 35±15 | 19 | 43±20 | 27 | 1.2 | 23±2 | 6 | 34±13 | 12 | 1.5 |
| | p.Arg396Cys/p.Arg194Cys | 58±8 | 78 | 66±10 | 66 | 1.1 | 69±8 | 61 | 51±13 | 50 | 0.7 |
| | p.Tyr114His/p.Thr242Ile | 60±8 | 70 | 60±11 | 72 | 1.0 | 71±16 | 48 | 50±18 | 46 | 0.7 |
| Type I. | p.Arg426His/p.Ser23Arg | 67±20 | 82 | 96±11 | 98 | 1.4 | 39±17 | 20 | 61±20 | 28 | 1.6 |
| | p.Asp268Asn/p.Arg194Cys | *not done because of permanent and profound loss of kanamycin resistant p.Asp268Asn construct* | | | | | | | | | |
| | p.Pro467Arg/p.Asp268Asn | *not done because of permanent and profound loss of kanamycin resistant p.Pro467Arg construct* | | | | | | | | | |
| | p.Arg426His/p.Arg426His[a] | 92±30 | 92 | 89±30 | 89 | 1.0 | 12±11 | 12 | 11±10 | 11 | 0.9 |
| | p.Asp215His/p.Ile351Thr | 133±28 | 139 | 106±33 | 121 | 0.8 | 101±30 | 133 | 103±39 | 99 | 1.0 |
| Type II. | p.Arg426His/p.Asp268His | 44±4 | 49 | 58±13 | 54 | 1.3 | 28±11 | 12 | 24±12 | 9 | 0.9 |
| | p.Arg426His/p.Thr450Ser | 73±10 | 87 | 78±17 | 78 | 1.1 | 16±6 | 13 | 19±5 | 14 | 1.2 |
| | p.Tyr114His/p.Arg190Gln | 121±29 | 93 | 92±21 | 78 | 0.8 | 98±18 | 77 | 93±42 | 64 | 0.9 |
| | p.Glu80Asp/p.Asp87Glu | 119±30 | 98 | 97±16 | 97 | 0.8 | 116±18 | 100 | 94±41 | 84 | 0.8 |
| | p.Arg426His/p.Asp430Asn | 88±10 | 115 | 112±32 | 120 | 1.3 | 56±14 | 54 | 71±20 | 55 | 1.2 |
| | p.Arg303Cys/p.Arg303Cys[a] | 18±1 | 18 | 44±13 | 44 | 2.4 | 20±2 | 20 | 43±9 | 43 | 2.1 |

Complexes were reconstituted at 25 and 50°C and their activities were measured with both of ADSL substrates, S-AMP and SAICAR, at 37°C. Mutations are ordered as they correspond to neonatal, type I and type II phenotypic groups. Combination of mutant proteins is provided in the form M1kan/M2amp where M1kan and M2amp define which mutation was expressed from kanamycine and ampicilin resistant vector.

[a]Denotes cases where homozygous mutant proteins were expressed from ampicilin resistant constructs only.

[b]Calc represent arithmetic means of the corresponding homomeric enzyme activities reported in Table 2.

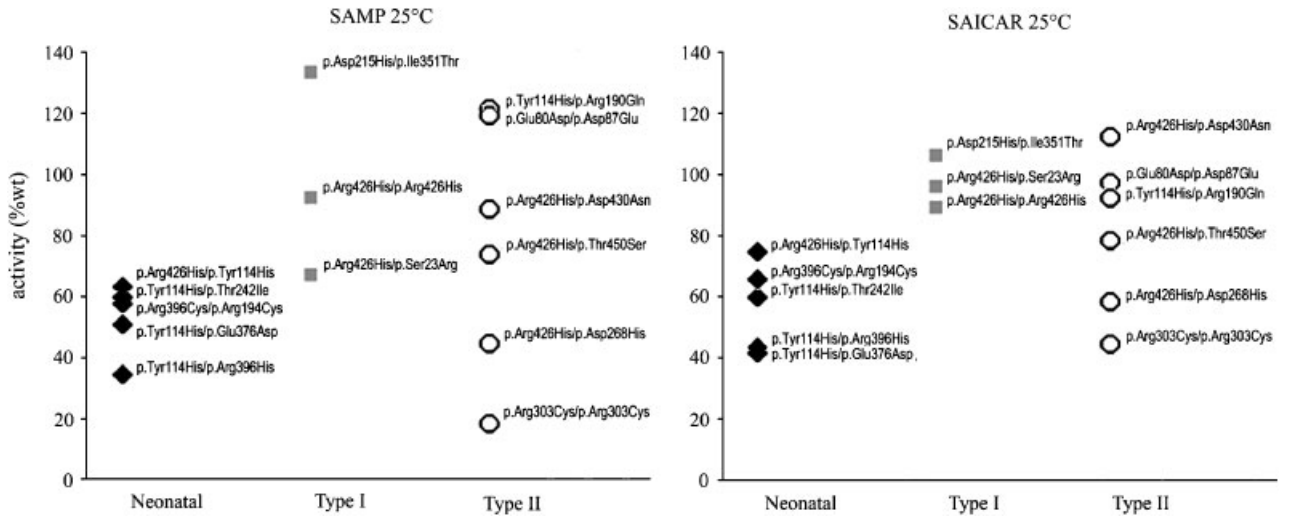


**Figure 3.** ADSL activities of heteromeric enzyme complexes as associated with individual phenotypic groups.

compared to the wild-type and all the other mutant proteins; (2) proteins with low residual activity (p.Tyr114His, p.Asp268His, p.Glu376Asp, p.Arg396Cys, and p.Arg396His); (3) thermally unstable proteins with high residual activity (p.Ser23RArg, p.Arg426His, and p.Thr450Ser); and (4) thermally stable proteins with normal or even higher enzyme activity (p.Glu80Asp, p.Asp87Glu, p.Arg190Gln, p.Arg194Cys, p.Asp215His, p.Thr242Ile, p.Ile351Thr, and p.Asp430Asn). Structural correlations within these classes allowed the following conclusions. (1) The p.Arg303Cys mutation is located directly in the active site where it causes a loss of positive charge of the Arg303 residue responsible for binding the substrate phosphate and reduces the reaction velocity of the enzyme toward both substrates (Fig. 4A). Why the reduction in reaction velocity is more pronounced for S-AMP cannot be satisfactorily explained using the static crystal structure because the spatial arrangement of the ADSL complex was solved with S-AMP but not with SAICAR. (2) All of the mutations associated with low residual activity affect residues involved in either the formation of catalytic sites (p.Tyr114His, p.Asp268His, p.Glu376Asp) or substrate channeling, which is mediated by positively charged residues (p.Arg396Cys, p.Arg396His) (Fig. 4B). (3) Neither of the thermally unstable proteins with higher residual activity has a mutation located directly in an active site or in the region involved in substrate binding. These mutated residues instead have an impact on protein stability. Mutations p.Ser23Arg and p.Thr450Ser (to lesser extent) incorporate steric changes of amino acid residues buried inside the protein core. The p.Ser23Arg mutation causes overpacking together with charge changes at the interface between the central helical region and the catalytic sites, whereas the p.Thr450Ser mutation affects the formation of the substrate channel as the amino acid exchange leads to cavity creation at a buried site. The p.Arg426His mutation is located at the surface of the substrate channel where its presence disrupts arginine-mediated interactions with Gln409 and Asp422 residues. This leads to reduced protein stability (Fig. 4C). (4) Mutations associated with normal enzyme activity are mostly structurally benign, as demonstrated by isomorphic exchanges (p.Glu80Asp and p.Asp87Glu), changes that do not influence stabilizing interactions (p.Asp215His, p.Asp430Asn) and changes that do not involve major steric effects (p.Thr242Ile, p.Ile351Thr). Although normally active, two mutations (p.Arg190Gln and p.Arg194Cys) were predicted to reduce protein stability because the loss of the positive charge disrupts electrostatic interactions in the central helical region (p.Arg190Gln) or at a subunit interface (p.Arg194Cys). A summary of the predicted structural effects and putative functional consequences of all of the analyzed mutations is provided in Table 4.

## Functional–Structural Correlation of Heteromeric Complexes

To assess the complementation effects of individual subunits in heteromeric mutant proteins, we calculated complementation coefficients (CC) defined as the ratio of the measured enzymatic activity over the arithmetic mean of the corresponding homomeric enzyme activities for each of the heteromeric complexes. Complementation coefficients were calculated for complexes equilibrated at both 25 and 50°C and for each of the substrates separately. The complementation coefficients obtained for complexes equilibrated at 25°C, which showed the effects of complementation on the catalytic properties of the enzyme, revealed three heteromeric complexes with a positive complementation effect higher than 25% (as defined in [Yu and Howell, 2000]): p.Tyr114His/p.Glu376Asp (CC = 1.25 and 0.98 for S-AMP and SAICAR, respectively), p.Tyr114His/p.Arg396His (CC = 1.84 and 1.59 for S-AMP and SAICAR, respectively), and p.Tyr114His/p.Arg190Gln (CC = 1.30 and 1.18 for S-AMP and SAICAR, respectively). A negative complementation effect was seen in the case of the p.Arg396Cys/p.Arg194Cys complex (CC = 0.74 and 1.00 for S-AMP and SAICAR, respectively). The positive complementation effects observed at 25°C may result from random but parallel buildup of nonmutated (wild-type) and hypermutated active sites during the tetramerization process. The buildup of wild-type active sites may positively affect the activity of otherwise inactive or less active enzyme subunits (Fig. 4D). Structural correlations showed that wild-type active sites might evolve in p.Arg426His/p.Tyr114His, p.Tyr114His/p.Glu376Asp, p.Tyr114His/p.Arg396His, p.Arg426His/p.Ser23Arg, and p.Arg396Cys/p.Arg194Cys complexes and perhaps also in p.Arg426His/p.Tyr114His, and p.Asp215His/p.Ile351Thr complexes, although the latter two did not show a corresponding effect in vitro.

The complementation coefficients obtained for complexes equilibrated at 50°C were informative with regard to mutual cooperation of differently mutated subunits in tetramer stabilization

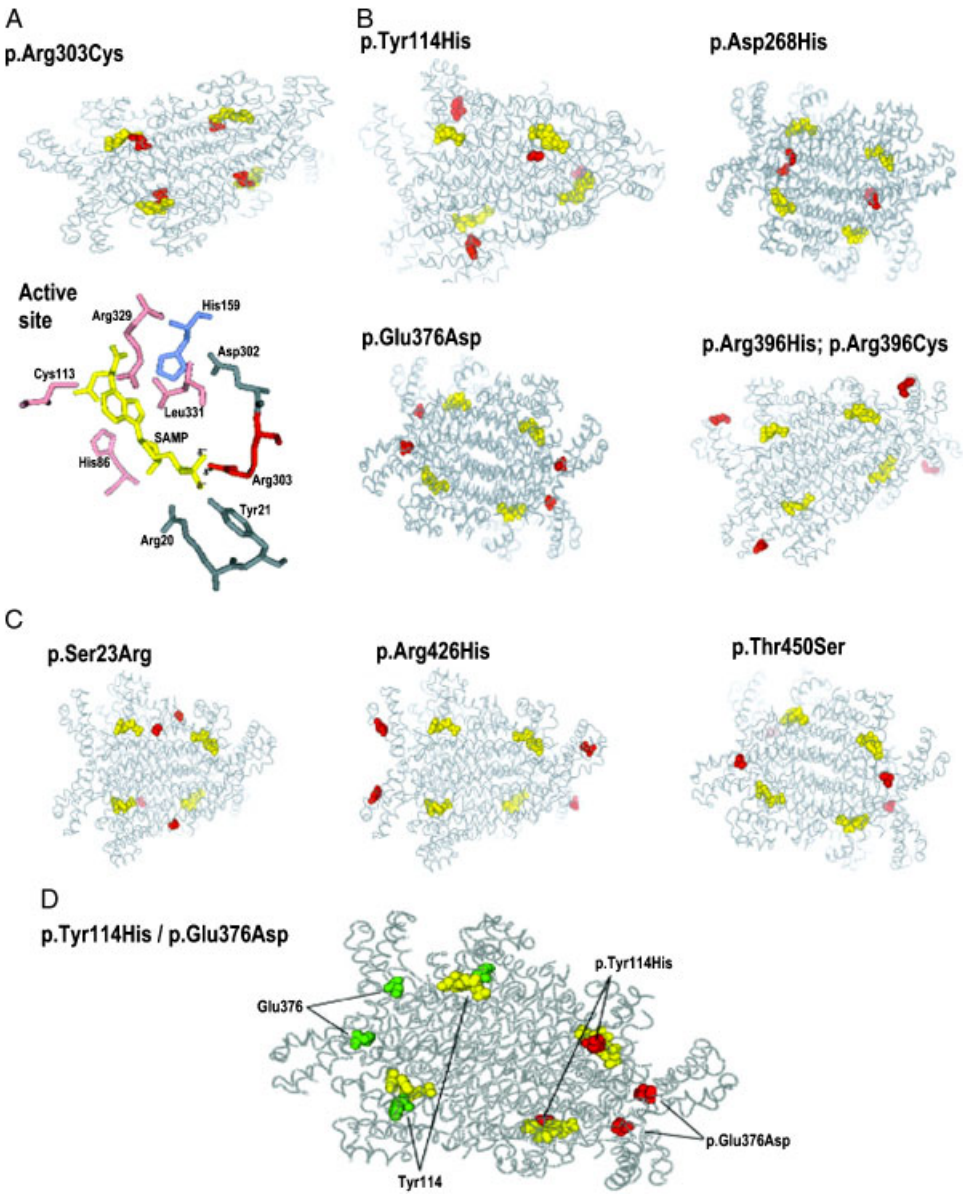


**Figure 4.** Location of the mutations in structural model of homotetrameric ADSL. Red or green balls represent mutated residues, yellow balls represent molecule of S-AMP. **A:** p.Arg303Cys mutation is located directly in the active site where it is in the immediate contact with S-AMP. Detail of one of the active sites demonstrating the effect of positive charge of the Arg303 residue on binding of the phosphate group of the substrate. **B:** Mutations associated with low residual enzyme activities affecting residues involved either in formation of catalytic sites (p.Tyr114His, p.Asp268His, p.Glu376Asp) or substrate channeling, which is mediated by positively charged residues (p.Arg396Cys, p.Arg396His). **C:** Mutations affecting thermal stability. Mutations p.Ser23Arg and p.Thr450Ser, both buried inside the protein globule and incorporating sterical changes of the amino acid residues. Mutation p.Ser23Arg causing overpacking together with charge changes located at the interface between central helical region and catalytic sites. Mutation p.Thr450Ser affects formation of the substrate channel due to creation of the cavity at the buried site. Mutation p.Arg426His located at the surface of the substrate channel. **D:** Build up of wild-type and hypermutated active sites during random tetramerization process demonstrated on case of p.Tyr114His/p.Glu376Asp heteromeric complex. Nonmutated residues forming wild-type active sites are shown as green balls; mutated residues forming hypermutated active sites are shown as red balls.

and were most pronounced in complexes p.Tyr114His/p.Glu376Asp (CC = 4.55 and 2.54 for S-AMP and SAICAR, respectively), p.Tyr114His/p.Arg396His (CC = 3.83 and 2.83 for S-AMP and SAICAR, respectively), and p.Arg426His/p.Asp268His (CC = 2.33 and 2.67 for S-AMP and SAICAR, respectively). A smaller positive complementation effect was also observed for the p.Tyr114His/p.Thr242Ile, p.Arg426His/p.Ser23Arg, and p.Tyr114His/p.Arg190Gln complexes. A negative complementation effect was not found for any of the analyzed heteromeric complexes. For the majority of the complexes, the stabilization effects could be attributed to the formation of nonmutated (wild-type) active sites during the tetramerization process (see above). We cannot exclude, however, that other stabilization factors such as positive intersubunit cooperation are involved. This could not be elucidated from analysis of the available ADSL crystal structure.

## Discussion

In this study we tried to identify a biochemical and structural basis for the phenotypic heterogeneity (e.g., different S-Ado/SAICAr

**Table 4. Location, Structural Impact, and Putative Functional Consequences of Analyzed ADSL Mutations**

| Mutation | Location in ADSL complex | Structural impact of mutation | Putative functional consequences |
|---|---|---|---|
| p.Ser23Arg | Central helical region/active site | Overpacking/charge change at buried site | Protein instability/deformation of catalytic cleft |
| p.Glu80Asp | Active site | Isomorphic change | Structurally benign |
| p.Asp87Glu | Active site | Isomorphic change | Structurally benign |
| p.Tyr114His | Active site | Charge and hydrophobicity change at buried site | Deformation of catalytic cleft |
| p.Arg190Gln | Central helical region | Charge change—loss of interaction with Asp129 | Protein instability |
| p.Arg194Cys | Subunit interface | Charge change—loss of interaction with Glu464/ hydrophobicity change at buried site/cavity creation | Protein instability |
| p.Asp215His | Substrate channel | Charge change and local changes at protein surface | Structurally benign |
| p.Thr242Ile | Active site | Minor local changes | Structurally benign |
| p.Asp268Asn | Active site | Charge change—loss of interaction with Lys264 | Deformation of catalytic cleft |
| p.Arg303Cys | Active site | Charge change—loss of interaction with substrate/ Creation of cavity | Deformation of catalytic cleft/affected substrate binding |
| p.Ile351Thr | Central helical region/active site | Minor local changes | Structurally benign |
| p.Glu376Asp | Active site /subunit interface | Isomorphic change/ Cavity creation—affected interaction with Lys276 | Deformation of catalytic cleft/protein instability |
| p.Arg396His/Cys | Substrate channel | Charge change—loss of interaction with Glu383 | Deformation and destabilization of the channel/affected channeling |
| p.Arg426His | Substrate channel | Charge change—affected interaction with Gln409 and Asp422 | Deformation and destabilization of the channel |
| p.Asp430Asn | Substrate channel | Charge change at protein surface | Structurally benign |
| p.Thr450Ser | Substrate channel | Cavity creation at buried site | Deformation and destabilization of the channel/protein instability |

Mutations are ordered according to their position in ADSL sequence.

ratios) present among patients with ADSL deficiency. To that end, we selected 16 genotypes representing three major clinical phenotypes of the disease and cloned individual mutations. We then expressed, purified, reconstituted, and characterized individual mutant proteins. Given the compound heterozygosity present in most of the studied cases and considering the tetrameric structure of the ADSL enzyme complex, we also used intersubunit complementation and prepared and characterized corresponding recombinant heteromeric mutant ADSL enzyme complexes. We assessed and tried to link the structural impact of the underlying mutations to the biochemical properties of the mutant proteins. From these functional–structural–phenotypic correlations, we can draw the following conclusions:

1. Different S-Ado/SAICAr ratios do not seem to result from disproportionate enzyme activity of the mutant protein complexes. In agreement with our previous studies [Jurecka et al., 2008; Kmoch et al., 2000; Mouchegh et al., 2007], we found that all except one of the mutant protein complexes, if active, displayed a proportional decrease in activity toward both of the enzyme substrates. The only exception to this was the p.Arg303Cys/p.Arg303Cys protein complex, which displayed a uniquely high SAICAR/S-AMP activity ratio. This finding could be directly linked to the steric changes in the active site of the p.Arg303Cys mutant enzyme, which probably affect the conversion of S-AMP more profoundly. It is interesting that this mutation has been identified in two patients with the mildest phenotypes and highest S-Ado/SAICAr ratios ever reported [Race et al., 2000].
2. The enzymatic activity of the heteromeric complexes correlated with the arithmetic mean of the corresponding homomeric enzyme activities. Supported by mass spectrometry data, this result shows that under "normal" conditions both mutant proteins contribute equally to tetramer and active site formation and that complementation effects are present.

As discussed above and contrary to our initial expectations, the complementation effects did not lead to the formation of unique catalytic sites in any of the studied heteromeric enzyme complexes, which would cause disproportionate activity and selectivity toward one of the enzyme substrates. Nevertheless, complementation had a positive effect on catalytic activity of some of the heteromeric complexes, probably due to the random buildup of wild-type active sites. The complementation effect was much more pronounced in heteromeric complexes equilibrated at 50°C, which suggests that the cooperation of differently mutated subunits also enhances enzyme complex stability, as observed in the p.Tyr114His/p.Glu376Asp, p.Tyr114His/p.Arg396His, p.Tyr114His/p.Thr242Ile, p.Arg426His/p.Ser23Arg, p.Arg426His/p.Asp268His, p.Tyr114His/p.Arg190Gln, and p.Glu80Asp/p.Asp87Glu heteromeric protein complexes using BN-PAGE and enzyme activity measurements.

Most importantly, the residual enzymatic activity and stability of the mutant enzyme complexes correlated with phenotype severity. This finding is also in agreement with and further corroborates our previous observations [Kmoch et al., 2000]. In other words, the phenotypic severity in ADSL deficiency probably reflects the degree of structural stability and residual enzyme activity of the corresponding ADSL enzyme complex. This can be documented best by the biochemical properties of the mutant proteins associated with the neonatal fatal phenotype. These proteins, notably, p.Tyr114His, p.Glu376Asp, p.Arg396Cys, p.Arg396His, and p.Arg426His, displayed the lowest residual activity and significant thermal instability in homomeric forms and in most of the heteromeric complexes they formed. These mutations also mostly affect residues forming the catalytic sites or residues involved in substrate channeling. Mutant proteins associated with moderate or mild disease displayed mostly normal enzymatic activity; the proteins were evidently stable, and the mutations seemed to be structurally benign based on in silico analysis of the ADSL structure. The pathogenic effects of these

biochemically benign and structurally stable mutations, therefore, are probably not related to their intrinsic structural and/or catalytic properties but rather to abnormalities that may manifest only under in vivo conditions inside eukaryotic cells. Such mutations may affect protein folding, slow down enzyme complex formation, and/or lead to accelerated degradation. These mechanisms may decrease the amount of otherwise normally functioning enzyme complex and lead to a much milder enzyme deficiency.

The question, however, is how the above findings can explain the different S-Ado/SAICAr ratio values observed in the cerebrospinal fluid and urine of individual patients. ADSL acts in two pathways of purine nucleotide metabolism: the de novo purine synthesis pathway and the purine nucleotide cycle. Although both pathways are constitutively active during development and throughout life [Flanagan et al., 1986; Swain et al., 1984; Van den Berghe et al., 1992; Watts, 1983], their activity must be precisely regulated and coordinated to meet the entirely different nucleotide demands of dividing, differentiating and fully differentiated cells. The regulation of purine metabolism certainly takes place at various levels as demonstrated by the distinct compartmentalization of the purinosome within cells [An et al., 2008] and the entirely different downstream regulatory effects of various intermediates of both of the pathways. It has been shown that SAICAR activates the expression of genes involved in de novo purine synthesis [Pinson et al., 2009; Rebora et al., 2001, 2005], and one can imagine that in case of ADSL deficiency, the accumulation of SAICAR may cause feedback activation of the de novo purine synthetic pathway, potentiating overall SAICAR production. In addition, ADSL complex instability, which is a characteristic feature of mutations associated with a severe phenotype, can also destabilize purinosome formation and may thereby contribute to a partial deficiency in purines. Combining these two mechanisms and presuming a relatively constant flux through the purine nucleotide cycle, it is reasonable to think that the phenotypic severity of ADSL deficiency is mainly determined by the ability of ADSL to channel SAICAR through the de novo purine pathway and the overall stability of the purinosome. One can envision that in dividing and differentiating (transcriptionally and proteosynthetically active) cells with a high demand for de novo purine synthesis, more profound defects in ADSL activity would probably result in significant purine nucleotide deficiency, SAICAR accumulation, and enhanced SAICAR and/or SAICAr-mediated toxicity. In a newborn with a more profound defect, brain maturation and overall development will be more severely affected and will present as the neonatal fatal form. At this stage the combination of activated de novo purine synthesis (more SAICAR production) and constant flux through the purine nucleotide cycle (constant amounts of S-AMP produced) would present biochemically as a low S-Ado/SAICAr ratio, particularly in the cerebrospinal fluid. In cases with less severe ADSL deficiency, however, relatively less SAICAR and more nucleotides will be produced, and patient development will not be as severely affected. The patient's brain would mature, and the demand for de novo purine synthesis in this organ would decreases accordingly. At this stage relatively less SAICAR will be produced, and in combination with a presumably constant amount of S-AMP being produced, this would present biochemically as a higher S-Ado/SAICAr ratio. Accordingly, we propose that the S-Ado/SAICAr ratio is not predictive of ADSL phenotype severity, but rather, that it is secondary to the patient's development and brain maturation (e.g., the age of the patient at the time of sample collection). Retrospective and/or prospective follow-up of S-Ado/SAICAr ratio values in individual cases, therefore, would be of great interest.

## Acknowledgments

This work was supported by a 301/07/0600 grant from the Czech Science Foundation. Institutional support was provided by the Ministry of Education of Czech Republic grants 1M6837805002 and MSM0021620806. The authors acknowledge Irena Sieglová for gel filtration measurements.

## References

An S, Kumar R, Sheets ED, Benkovic SJ. 2008. Reversible compartmentalization of de novo purine biosynthetic complexes in living cells. Science 320:103–106.

Ariyananda Lde Z, Lee P, Antonopoulos C, Colman RF. 2009. Biochemical and biophysical analysis of five disease-associated human adenylosuccinate lyase mutants. Biochemistry 48:5291–5302.

Brosius JL, Colman RF. 2002. Three subunits contribute amino acids to the active site of tetrameric adenylosuccinate lyase: Lys268 and Glu275 are required. Biochemistry 41:2217–2226.

Ciardo F, Salerno C, Curatolo P. 2001. Neurologic aspects of adenylosuccinate lyase deficiency. J Child Neurol 16:301–308.

Flanagan WF, Holmes EW, Sabina RL, Swain JL. 1986. Importance of purine nucleotide cycle to energy production in skeletal muscle. Am J Physiol 251 (5 Pt 1):C795–C802.

Fon EA, Demczuk S, Delattre O, Thomas G, Rouleau GA. 1993. Mapping of the human adenylosuccinate lyase (ADSL) gene to chromosome 22q13.1→q13.2. Cytogenet Cell Genet 64:201–203.

Gitiaux C, Ceballos-Picot I, Marie S, Valayannopoulos V, Rio M, Verrieres S, Benoist JF, Vincent MF, Desguerre I, Bahi-Buisson N. 2009. Misleading behavioural phenotype with adenylosuccinate lyase deficiency. Eur J Hum Genet 17:133–136.

Jaeken J, Van den Berghe G. 1984. An infantile autistic syndrome characterised by the presence of succinylpurines in body fluids. Lancet 2:1058–1061.

Jaeken J, Wadman SK, Duran M, Van Sprang FJ, Beemer FA, Holl RA, Theunissen PM, de Cock P, Van den Bergh F, Vincent MF, Van den Berghe G. 1988. Adenylosuccinase deficiency: an inborn error of purine nucleotide synthesis. Eur J Pediatr 148:126–131.

Jaeken J, Van den Bergh F, Vincent MF, Casaer P, Van den Berghe G. 1992. Adenylosuccinase deficiency: a newly recognized variant. J Inherit Metab Dis 15:416–418.

Jurecka A, Zikanova M, Tylki-Szymanska A, Krijt J, Bogdanska A, Gradowska W, Mullerova K, Sykut-Cegielska J, Kmoch S, Pronicka E. 2008. Clinical, biochemical and molecular findings in seven Polish patients with adenylosuccinate lyase deficiency. Mol Genet Metab 94:435–442.

Kmoch S, Hartmannova H, Stiburkova B, Krijt J, Zikanova M, Sebesta I. 2000. Human adenylosuccinate lyase (ADSL), cloning and characterization of full-length cDNA and its isoform, gene structure and molecular basis for ADSL deficiency in six patients. Hum Mol Genet 9:1501–1513.

Krijt J, Kmoch S, Hartmannova H, Havlicek V, Sebesta I. 1999. Identification and determination of succinyladenosine in human cerebrospinal fluid. J Chromatogr B Biomed Sci Appl 726:53–58.

Lee TT, Worby C, Bao ZQ, Dixon JE, Colman RF. 1999. His68 and His141 are critical contributors to the intersubunit catalytic site of adenylosuccinate lyase of *Bacillus subtilis*. Biochemistry 38:22–32.

Maaswinkel-Mooij PD, Laan LA, Onkenhout W, Brouwer OF, Jaeken J, Poorthuis BJ. 1997. Adenylosuccinase deficiency presenting with epilepsy in early infancy. J Inherit Metab Dis 20:606–607.

Mouchegh K, Zikanova M, Hoffmann GF, Kretzschmar B, Kuhn T, Mildenberger E, Stoltenburg-Didinger G, Krijt J, Dvorakova L, Honzik T, Zeman J, Kmoch S, Rossi R. 2007. Lethal fetal and early neonatal presentation of adenylosuccinate lyase deficiency: observation of 6 patients in 4 families. J Pediatr 150:57–61 e2.

Pinson B, Vaur S, Sagot I, Coulpier F, Lemoine S, Daignan-Fornier B. 2009. Metabolic intermediates selectively stimulate transcription factor interaction and modulate phosphate and purine pathways. Genes Dev 23:1399–1407.

Race V, Marie S, Vincent MF, Van Den Berghe G. 2000. Clinical, biochemical and molecular genetic correlations in adenylosuccinate lyase deficiency. Hum Mol Genet 9:2159–2165.

Rebora K, Desmoucelles C, Borne F, Pinson B, Daignan-Fornier B. 2001. Yeast AMP pathway genes respond to adenine through regulated synthesis of a metabolic intermediate. Mol Cell Biol 21:7901–7912.

Rebora K, Laloo B, Daignan-Fornier B. 2005. Revisiting purine-histidine cross-pathway regulation in *Saccharomyces cerevisiae*: a central role for a small molecule. Genetics 170:61–70.

Sivendran S, Patterson D, Spiegel E, McGown I, Cowley D, Colman RF. 2004. Two novel mutant human adenylosuccinate lyases (ASLs) associated with autism and characterization of the equivalent mutant *Bacillus subtilis* ASL. J Biol Chem 279:53789–55397.

Spiegel EK, Colman RF, Patterson D. 2006. Adenylosuccinate lyase deficiency. Mol Genet Metab 89:19–31.

Stone TW, Roberts LA, Morris BJ, Jones PA, Ogilvy HA, Behan WM, Duley JA, Simmonds HA, Vincent MF, van den Berghe G. 1998. Succinyl-purines induce neuronal damage in the rat brain. Adv Exp Med Biol 431: 185–189.

Strohalm M, Hassman M, Kosata B, Kodicek M. 2008. mMass data miner: an open source alternative for mass spectrometric data analysis. Rapid Commun Mass Spectrom 22:905–908.

Swain JL, Hines JJ, Sabina RL, Harbury OL, Holmes EW. 1984. Disruption of the purine nucleotide cycle by inhibition of adenylosuccinate lyase produces skeletal muscle dysfunction. J Clin Invest 74:1422–1427.

Valik D, Miner PT, Jones JD. 1997. First U.S. case of adenylosuccinate lyase deficiency with severe hypotonia. Pediatr Neurol 16:252–255.

Van den Bergh F, Vincent MF, Jaeken J, Van den Berghe G. 1993. Residual adenylosuccinase activities in fibroblasts of adenylosuccinase-deficient children: parallel deficiency with adenylosuccinate and succinyl-AICAR in profoundly retarded patients and non-parallel deficiency in a mildly retarded girl. J Inherit Metab Dis 16:415–424.

Van den Berghe G, Bontemps F, Vincent MF, Van den Bergh F. 1992. The purine nucleotide cycle and its molecular defects. Prog Neurobiol 39:547–561.

Van den Berghe G, Jaeken J. 1986. Adenylosuccinase deficiency. Adv Exp Med Biol 195(Pt A):27–33.

Van Keuren ML, Hart IM, Kao FT, Neve RL, Bruns GA, Kurnit DM, Patterson D. 1987. A somatic cell hybrid with a single human chromosome 22 corrects the defect in the CHO mutant (Ade-I) lacking adenylosuccinase activity. Cytogenet Cell Genet 44:142–147.

Watts RW. 1983. Some regulatory and integrative aspects of purine nucleotide biosynthesis and its control: an overview. Adv Enzyme Regul 21:33–51.

Wittig I, Braun HP, Schagger H. 2006. Blue native PAGE. Nat Protoc 1:418–428.

Yu B, Howell PL. 2000. Intragenic complementation and the structure and function of argininosuccinate lyase. Cell Mol Life Sci 57:1637–1651.

Zikanova M, Krijt J, Hartmannova H, Kmoch S. 2005. Preparation of 5-amino-4-imidazole-N-succinocarboxamide ribotide, 5-amino-4-imidazole-N-succinocarboxamide riboside and succinyladenosine, compounds usable in diagnosis and research of adenylosuccinate lyase deficiency. J Inherit Metab Dis 28:493–499.